Supporting Information

Newly Developed Poly(Allyl Glycidyl Ether/Divinyl Benzene) Polymer for Phosphopeptides Enrichment and Desalting of Biofluids

Muhammad Najam-ul-Haq[1*], Adeela Saeed[1,2], Fahmida Jabeen[1], Fernando Maya[2], Muhammad Naeem Ashiq[1], Ahsan Sharif[3]

[1]: Institute of Chemical Sciences, Bahauddin Zakariya University, Multan 60800, Pakistan.

[2]: The Molecular Foundry, E.O. Lawrence Berkeley National Laboratory, Berkeley, CA 94720, USA

[3]: Institute of Chemistry, University of the Punjab, Quaid-i-Azam Campus, Lahore 54590, Pakistan.

* Corresponding Author

Dr. M. Najam-ul-Haq
Institute of Chemical Sciences
Bahauddin Zakariya University
Multan 60800
Pakistan
Tel.: +92 306 7552653
Fax: +92 61 9210138
Email: najamulhaq@bzu.edu.pk

Keywords: Polymerization, IMAC (immobilized metal ion affinity chromatography), Reversed Phase, Phosphopeptides, Tryptic digests, Desalting, MALDI-MS, Selectivity

Chemicals and Materials

Allyl Glycidal Ether (AGE) technical grade, ≥90% (GC), divinyl benzene (80%, technical grade, Sigma-Aldrich), were used as the monomers. 2,2′-Azobis(2-methylpropionitrile) (98%, Sigma-Aldrich) was used as an initiator. All monomers were purified by passing through a bed of basic alumina to remove the inhibitors. Acetonitrile (ACN), trifluoroacetic acid (TFA, analytical reagent grade), methanol (HPLC, ≥ 99.9%), ammonium hydrogen carbonate (NH_4HCO_3), iodoacetamide (IAA), dithiothreitol (DTT), 2,5-dihydroxybenzoic acid (DHB) were purchased from Sigma-Aldrich and used as received. Trypsin (bovine pancreas), bovine serum albumin (BSA) and casein (bovine milk) were obtained from Sigma-Aldrich. Dichloromethane and the base triethylamine were purchased from Fluka. Protein Calibration Standard-I was bought from Bruker Daltonics Inc. (Bremen, Germany).

Instrumentation

Nitrogen adsorption/desorption isotherms and pore size distributions were measured using an ASAP 2020 surface area and porosimetry analyzer (Micromeritics, Norcross, GA). Scanning electron micrographs (SEM) and energy dispersive X-ray (EDX) spectra of polymer were obtained using a Zeiss Gemini Ultra Field-Emission Scanning Electron Microscope (Peabody, MA, USA) integrated with an energy dispersive X-ray spectrometer (Thermo Electron, USA). FT-IR spectra of the bulk polymer were acquired using a Spectrum One IR instrument (Perkin Elmer, Waltham, MA, USA). Mass spectra were obtained by using Bruker Autoflex II MALDI-TOF/TOF-MS.

Protein Digestion

For digestion, 2 mg of each protein was dissolved in 1 mL of water and the solution was aliquoted to 200 μL fractions. To each fraction 160 μL of ammonium hydroxide and 50 μL of dithiothreitol were added. The fractions were incubated at 50 °C in a thermomixer for 15 min.

The solution was cooled down to room temperature by the gradual addition of 50 µL iodoacetamide solution. The solution was incubated in dark for 15 min. 1000 µL of deionized water was then added, followed by the addition of 2 µg trypsin. The solution was digested in a thermomixer at 37 °C for 14 hours. The digestion was stopped by acidifying the solution with 10 µL 1% TFA and placed in the thermomixer for 5 min. The digested proteins were stored at -20 °C. For the non-fat milk and egg yolk, 500 µL was digested using the same procedure as the other fractions of protein solution.

Serum digestion was carried out using 20 µL of serum sample. After reduction and alkylation, the solution was diluted using 50 mM NH_4HCO_3 to make up the volume up to 700 µL. Trypsin was added (2 µg/µL) in the ratio of 1:50 and digestion was carried out at room temperature overnight. 1% TFA was used to quench the digestion.

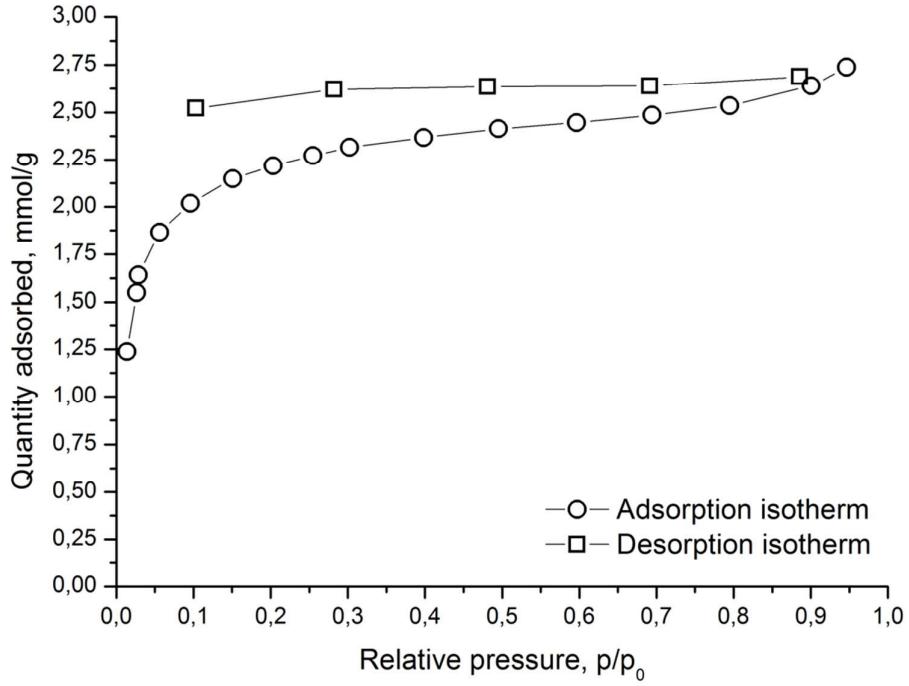

Figure S1: Nitrogen adsorption porosimetry on poly(AGE/DVB).

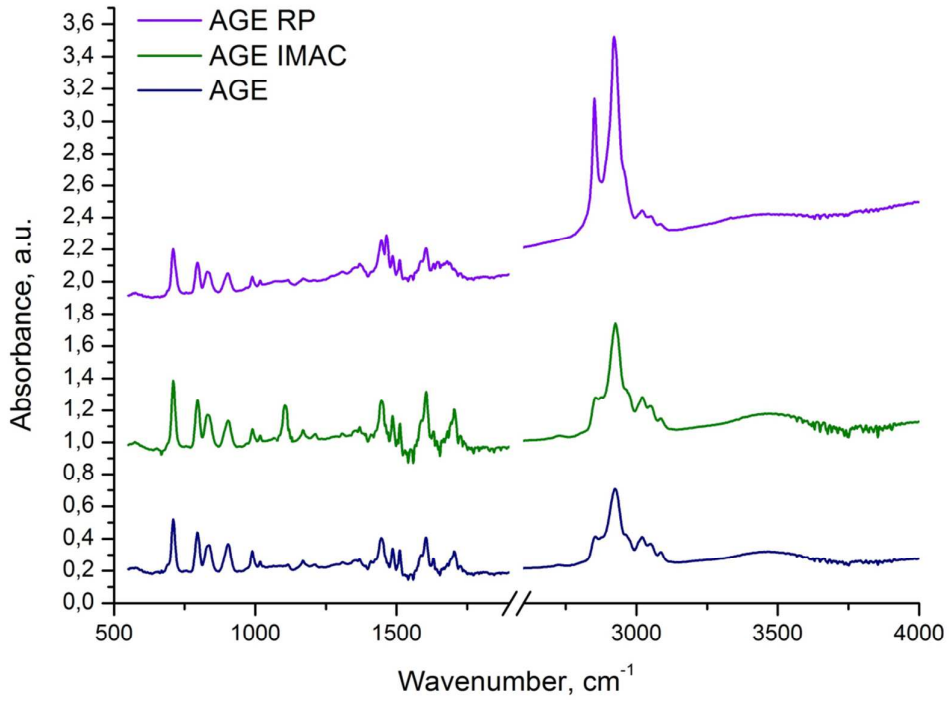

Figure S2: FT-IR spectra of (a) poly(AGE/DVB) (b) poly(AGE/DVB)-IMAC and (c) poly(AGE/DVB)-RP.

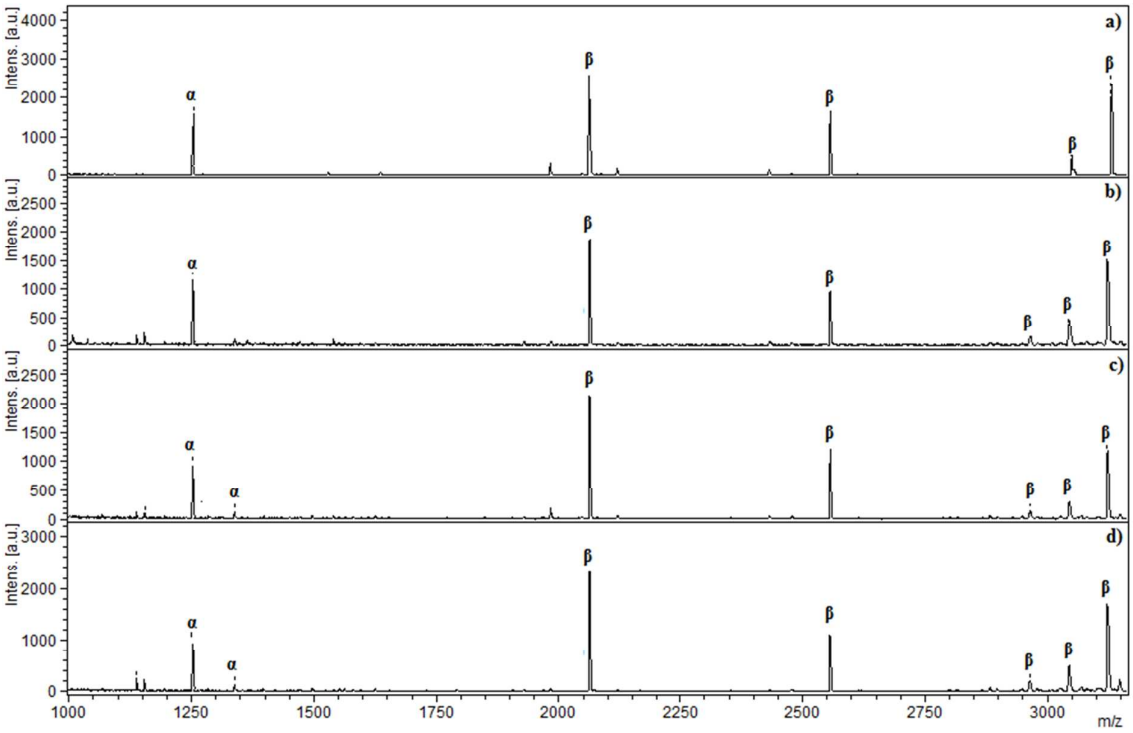

Figure S3: Comparison of enrichment efficiency of different metal ions immobilized on poly(AGE/DVB)-IMAC using tryptic β-casein digest as sample. (a) poly(AGE/DVB)-IMAC-Fe^{3+} (b) poly(AGE/DVB)-IMAC-La^{3+} (c) poly(AGE/DVB)-IMAC-Eu^{3+} and (d) poly(AGE/DVB)-IMAC-Er^{3+}.

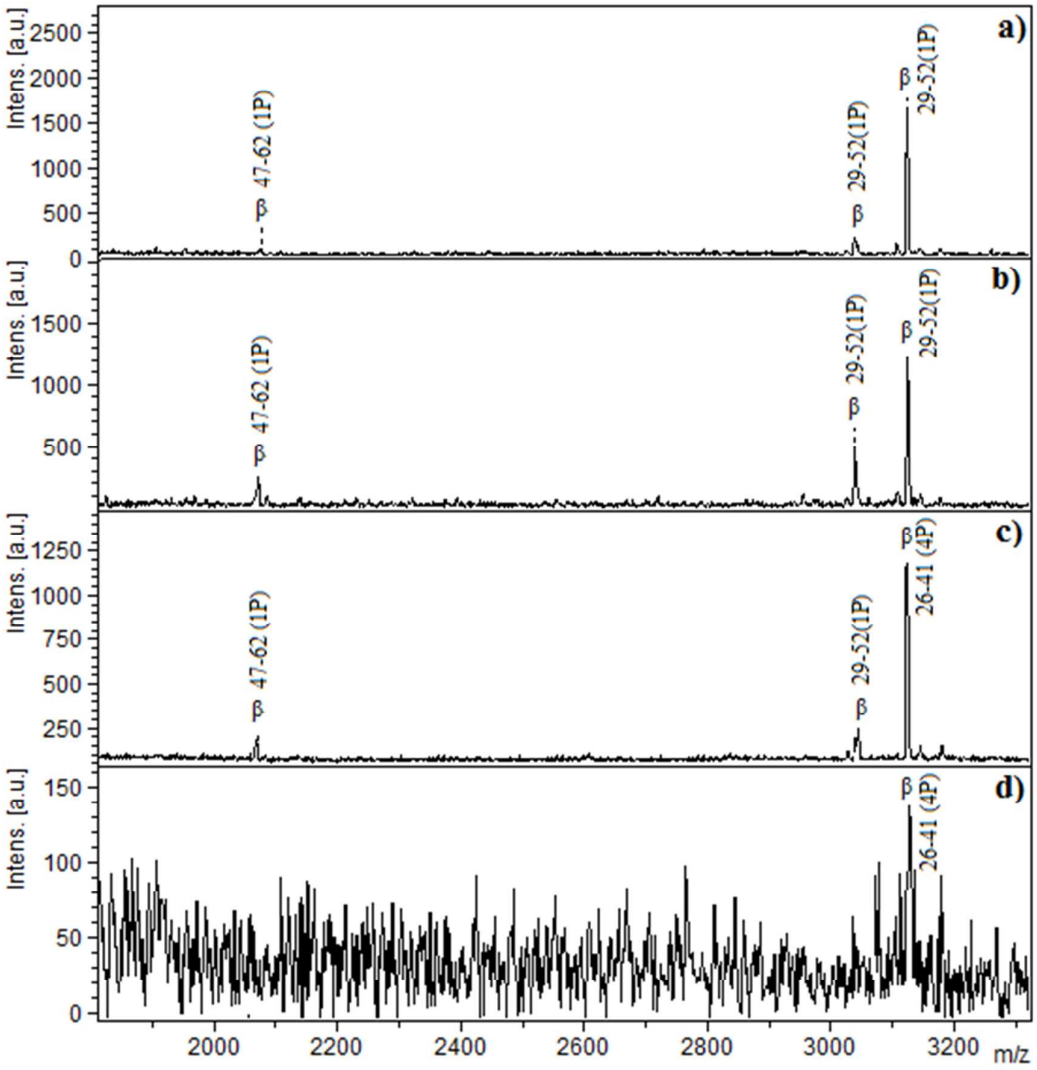

Figure S4: MALDI-MS spectra showing high selectivity of poly(AGE/DVB)-IMAC using spiked de-phosphorylated HeLa cell extract in different ratio: (a) 1:500 (b) 1:1000 (c) 1:1500 (d) 1:2000. Identified phosphopeptides are labelled as β with their number of phosphorylated groups and amino acid position.

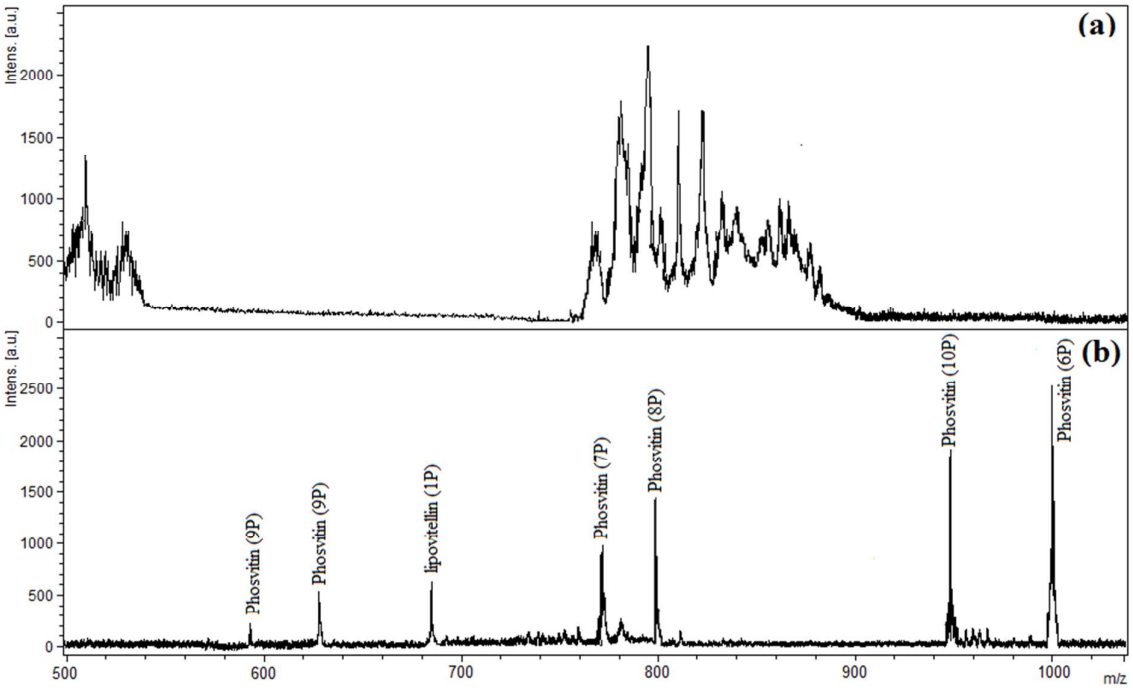

Figure S5: MALDI-MS spectra of (a) egg yolk digest without enrichment (b) eluted fraction after enrichment with poly(AGE-DVB)-IMAC-Fe^{3+}.

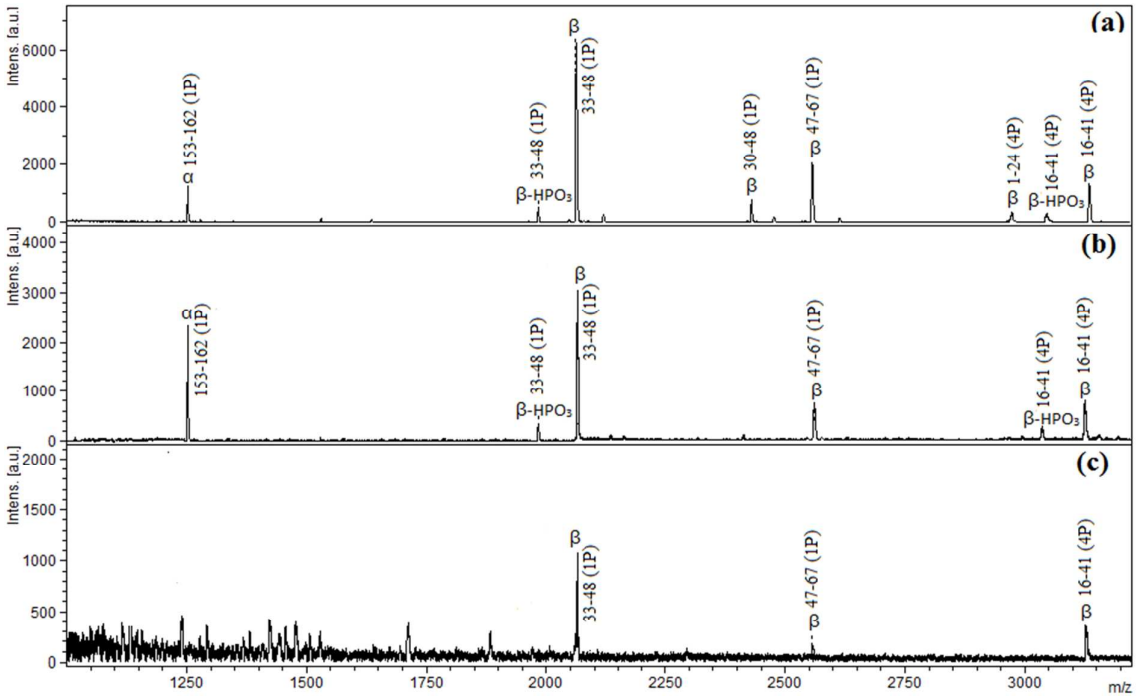

Figure S6: MALDI-MS spectra of different concentrations of β-casein digest enriched on poly(AGE-DVB)-IMAC-Fe^{3+} (a) 100 fmol (b) 50 fmol (c) 2 fmol. Identified phosphopeptides are labelled with amino acid position and number of phosphate groups.

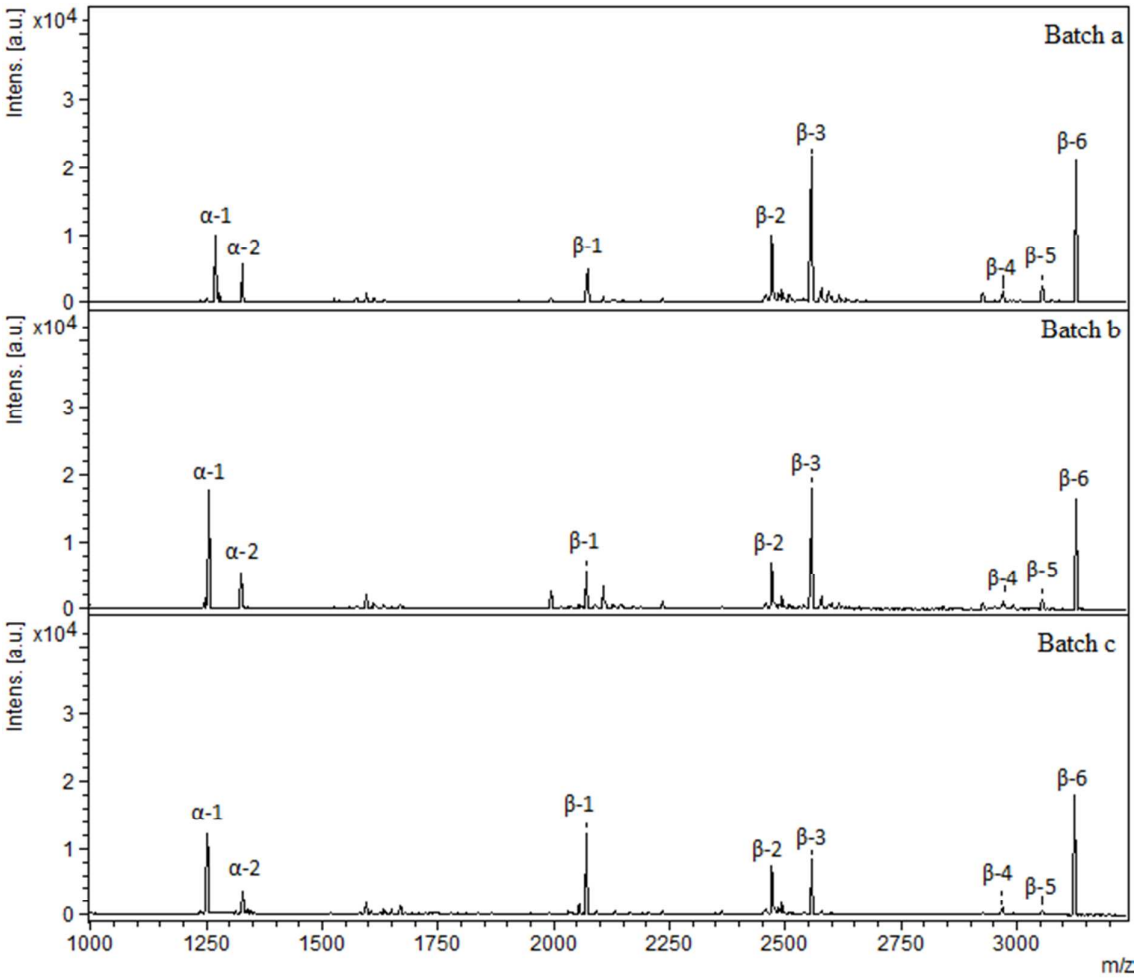

Figure S7: Measurement of reproducibility using poly(AGE/DVB)-IMAC-Fe^{3+} for β-casein digest. The calculated SD is given in Table S3.

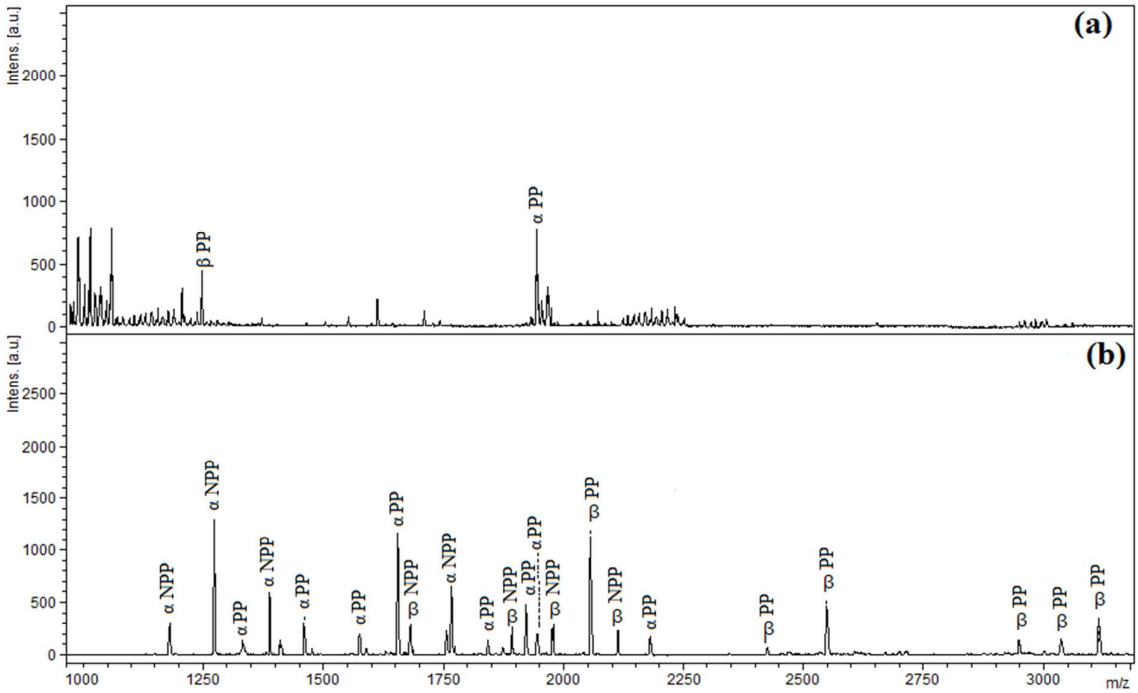

Figure S8: MALDI-MS spectra showing desalting of non-fat milk digest by poly(AGE-DVB)-RP. Identified peptides are labelled with α and β, based on their origin. Symbols PP and NPP show phosphorylated and non-phosphorylated peptides respectively.

Table S1: Summary of nitrogen adsorption porosimetry studies on Poly(AGE/DVB)

Surface Area	
Single point surface area at p/p° = 0.203435507	172.3831 m^2/g
BET Surface Area	173.1554 m^2/g
t-Plot Micropore Area	92.3524 m^2/g
t-Plot External Surface Area	80.8030 m^2/g
BJH Adsorption cumulative surface area of pores between 17.000 Å and 3000.000 Å width	72.369 m^2/g
BJH Desorption cumulative surface area of pores between 17.000 Å and 3000.000 Å width	25.9253 m^2/g
Pore Volume	
Single point adsorption total pore volume of pores less than 207.716 Å width at p/p°= 0.900603762	0.091519 cm^3/g
t-Plot micropore volume	0.041105 cm^3/g
BJH Adsorption cumulative volume of pores between 17.000 Å and 3000.000 Å width	0.051220 cm^3/g
BJH Desorption cumulative volume of pores between 17.000 Å and 3000.000 Å width	0.015069 cm^3/g
Pore Size	
Adsorption average pore width (4V/A by BET)	21.1416 Å
BJH Adsorption average pore width (4V/A)	28.310 Å
BJH Desorption average pore width (4V/A)	23.249 Å

Table S2: Identified phosphopeptides from tryptic serum digest enriched by poly(AGE/DVB)-IMAC-Fe^{3+}. Identification carried out by using mascot search. Phosphorylation identification by Phosphosite plus.

Peak Label	Phosphopeptide Sequence	Protein	Accession No.
p1	GS*LHVWK	Minor histocompatibility protein	HMHB1_HUMAN
p2	ET*IEQEK	Thymosin beta-10	TYB10_HUMAN
p3	KT*NT*EEK	Thymosin beta-15A	TB15A_HUMAN
p4	S*WFS*GCF	Keratin-associated protein 22-1	KR221_HUMAN
p5	MT*TSFQQR	Putative uncharacterized protein	YT006_HUMAN
p6	RNFDT*LDLPKR	Armadillo repeat protein deleted in velo-cardio-facial syndrome	O00192_HUMAN
p7	VT*PDS*AVWAP	Putative uncharacterized protein C14orf144	CN144_HUMAN
p8	KEY*KCT*SCKK	Putative metallothionein MT1DP	A1L3X4_HUMAN
p9	MCSY*YHMKK	IgA-inducing protein homolog	IGIP_HUMAN
p10	RGS*FSSENTWRK	Alkylated repair protein AlkB homolog 5	Q6P6C2_HUMAN
p11	ELQPS*EEVT*WK	NADH dehydrogenase [ubiquinone] 1 beta subcomplex subunit	NDUB1_HUMAN
p12	KLKDLFDYS*PPLHKN	Bcl-2-associated transcription factor 1	Q9NYF8_HUMAN
p13	RS*SSRS*S*SPSSSRSRS	Bcl-2-associated transcription factor 1	O95218_HUMAN
p14	RTLDRS*GDLGDMEPLKG	p120 catenin	O00716_HUMAN
p15	RNWTEDMEGGISS*PVKKT	Nuclear factor 1-C type	P08651_HUMAN
p15	RRSS*DSWEVWGSASTNRN	ADP-ribosylation factor GTPase activating protein 1	Q8N6T3_HUMAN
p16	MCT*T*LFLLS*TLAMLWRR	Progressive rod-cone degeneration protein	Q00LT1_HUMAN
p17	RAAS*LNYLNQPSAAPLQVSR G	Kinesin-like protein 8	Q9NSK0_HUMAN
p18	RAEGEWEDQEALDYFS*DKE	Bcl-2-associated transcription factor 1	Q9NYF8_HUMAN
p19	RS*ASSASSLFSPSSTLESS*SR L	Pumilio homolog 1	Q14671_HUMAN
p20	RRGS*GDTSSLIDPDTSLSE	Leucine-rich repeat flightless interacting protein	Q9Y608_HUMAN

p21	KQSSQAETDS*MSLSEKS*RK V	Nuclear interacting partner of ALK	Q86WB0_HUMAN
p22	KVVDYSQFQES*DDADEDYG RD	Nuclear ubiquitous casein and cyclin-dependent kinase substrate 1	Q9H1E3_HUMAN
p23	REFLESQEDY*DPCWS*LQEK Y	ADP-ribosylation factor GTPase-activating protein 1	Q8N6T3_HUMAN
p24	KSLS*DSESDDSKS	Chromobox protein homolog 3	Q13185_HUMAN
p25	KIYHLDAES*DEDEDFKEQTR L	Neural precursor cell expressed developmentally down-regulated protein 5	Q15019_HUMAN
p26	RENVEYIEREES*DGEYDEFG RK	Zn-finger Ran-binding domain containing protein 2	O95218_HUMAN
p27	RSILTSLLLNSS*QSS*T*S*SEE TVLRS	TIF1-alpha	O15164_HUMAN
p28	RRPAPAVS*PGSWKP	Zn finger protein KIAAI802	Q96JM3_HUMAN
p29	KPDSEDLSSQSS*AS*KASQED ANEIKS	Ubiquitin-protein ligase BEEI-A	Q5VTRS_HUMAN
p30	KLTVENS*PKQEAGISEGQGT AGEEEEKK	Protein DRPI	Q43583_HUMAN
p31	KLNHVAAGLVS*PSLKS	Splicing factor Arg/Ser Rich 11	Q05519_HUMAN
p32	RDGTAPPPQSPGSPTGQDEEW S*DEESPRK	Protein kinase and casein kinase substrate in neurons protein 3	Q9UKS6_HUMAN
p33	KDMS*PLSETEMALGKD	Microtubule-associated protein 4 (MAP 4)	P27816_HUMAN
p34	KWAHDKFS*GEEGEIEDDESG T*ENREEKD	Catenin-alpha	P35221_HUMAN
p35	RYQDEVFGGFVTEPQEES*EE EVEEPEERQ	G3BP-1	Q13283_HUMAN
p36	KNRPTS*ISWDGLDSGKL	Phosphatidylethanol-amine binding protein (PEBP-1)	P30086_HUMAN
p37	RAS*GEMASAQYITAALRD	Ubiquitin carboxyl terminal hydrolase 14	P54578_HUMAN
p38	IIFVLLLS*GIVSISASSTTGVA MHTSTSSSVTK	Glycophorin-E	GLPE_HUMAN
p39	GPPGDEEPLEGPELHVLMINA PS* VLAGFS*NAS*	Putative uncharacterized protein encoded by LINC00334	NC334_HUMAN
p40	MS*PPSSMCSPVPLLAAASGQ NRMTQGQHFLQK	Putative tumor antigen NA88-A	CT18_HUMAN
p41	T*LPLLT*LQMDLLPPNPAPS* LPPPS*LPTGHLGR	Putative uncharacterized protein PRO1768	YN005_HUMAN
p42	MSY*SGSY*Y*GGLGYGCGGF GGLGYGYSCGCGSFR	Keratin-associated protein 19-7	KR197_HUMAN
p43	S*PLQLQTVIY*RLIVQIQHLNI	Leucine zipper protein 6	LUZP6_HUMAN

	PSSSSTHSSPF		
p44	KTQT*PPVSPAPQPTEERL	Src substrate cortactin (Amplaxin) oncogene EMSI	Q14247_HUMAN
p45	GGSSY*PSNLVY*STEPLISQH LPAGFLSLQGLSGDLLGNP	Keratin-associated protein 23-1	KR231_HUMAN
p46	MKFFMVLLPAS*LAS*T*S*LA ILDVESGLLPQLSVLLSNRL	Putative glycosylation-dependent cell adhesion molecule 1	Q8IVK1_HUMAN
p47	KTIGGDDS*FNTFFSETGAGK H	Alpha-tubulin 6	Q9BQE3_HUMAN
p48	MKLS*GMFLLLS*LALFCFLT* GVFSQGGQVDCGEFQDPK	Serine protease inhibitor Kazal-type 6	ISK6_HUMAN
p49	FFMVLLPAS*LAS*T*S*LAILD VES*GLLPQLSVLLSNRLR	Putative glycosylation-dependent cell adhesion molecule 1	GLCM1_HUMAN
p50	RHSTAS*NSS*NLSSPPS*PASR K	Ser/Thr-protein kinase NRCK α	Q5VT25_HUMAN
p51	RS*LAADDEGGPELEPDYGTA RR	Armadillo repeat protein deleted in velo-cardio-facial syndrome	O00192_HUMAN
p52	HVLNLY*LLGVVLTLLSIFVR VMESLEGLLESPSPGTSWTTR	Hypoxia-inducible lipid droplet-associated protein	HLPDA_HUMAN

Table S3: Selected m/z values of three enrichment analysis showing the reproducibility of characteristic phosphopeptides derived from β-casein using poly(AGE/DVB)-IMAC-Fe^{3+}.

Selected m/z	Batch A	Batch B	Batch C	Standard Deviation
α-1	1254.018	1254.871	1254.644	0.441
α-2	1329.470	1329.173	1330.112	0.389
β-1	2061.264	2061.891	2061.877	0.219
β-2	2473.348	2473.161	2473.173	0.104
β-3	2556.821	2556.002	2556.608	0.424
β-4	2969.752	2969.990	2970.292	0.370
β-5	3054.075	3054.185	3054.387	0.158
β-6	3122.775	3122.806	3122.904	0.067

Table S4: Comparison of poly(AGE/DVB)-IMAC-Fe^{3+} with literature regarding selectivity, sensitivity and number of enriched phosphopeptides. Only the polymer-based strategies are included in the comparison.

Materials	Number of enriched Phosphopeptides from standard	Selectivity	Sensitivity	Ref.
Fe(III)-NTA-PHEMA-Modified Plates	3	-	15 fmol	1
$ZrPO_3^-$ modified MALDI target	4	1:10	1 fmol	2
Ti^{4+}-NTA PEG/MNP	2	20:1000	20 fmol	3
Fe_3O_4/poly(GMA-co-EDMA) monolith	3	-	-	4
Fe_3O_4/poly(VPA-EDMA-1)-Zr^{4+})	3	1:100	3 pmol	5
Fe_3O_4 coated poly poly(HEMA-co-EDMA)	6	-	-	6
poly(GPE/DVB)-La^{3+}	8	1:10	1 fmol	7
poly(AGE/DVB)-Fe^{3+}	*10*	*1:2000*	*2 fmol*	*present study*

Table S5: Comparison of poly(GPE/DVB)-IMAC/RP to poly(AGE/DVB)-IMAC/RP

	Investigated studies	**Poly(GPE/DVB)**	**Poly(AGE/DVB)**	**Effect on enrichment**
Polymer characteristics	Surface area	89.3824 m^2/g	173.1554 m^2/g	Increase in selectivity
	Adsorption average pore width	20.8111 Å	21.1416 Å	Better adsorption
IMAC based phosphopeptides enrichment	Feasibility (standard)	8 phosphopeptides	10 phosphopeptides	High number of phosphopeptides
	Selection of metal ion	La^{3+}	Fe^{3+} Comparison to La^{3+}/ Eu^{3+}/Er^{3+}	Conventional metal ion, Fe^{3+}, is used to address the material role in enrichment and to overcome Fe based acidic peptides
	Selectivity	10 folds complexity level achieved	2000 folds complexity level achieved	Attributed to high surface area of polymeric IMAC which distinguish it from poly(GPE/DVB)
	Milk sample	8 α-casein and 6 β-casein phosphopeptides	12 α-casein and 8 β-casein phosphopeptides	Increase in number of phosphopeptides which prove the high selectivity
	Egg yolk	6 phosphorylated peptides (up to 9P)	7 multi phosphorylated peptides (up to 10P)	Better enrichment of multi phosphopeptides
	Serum profiling	Fibrinogen based study for ovarian carcinoma	52 different phosphopeptides along with fibrinogen phosphopeptides	Characteristic fibrinogen phosphopeptides are enriched by both IMAC materials, one with target study in relevance to ovarian carcinoma whereas in case of poly(AGE/DVB)-IMAC serum profiling is done using control sample
RP based desalting	Desalting Casein mixture	26 peptides	31 peptides	Ensure better pre-concentration of sample with high number of enriched content

References

(1) Dunn, J. D.; Igrisan, E. A.; Palumbo, A. M.; Reid, G. E.; Bruening, M. L. Phosphopeptide Enrichment Using MALDI Plates Modified with High-Capacity Polymer Brushes. *Anal. Chem.* **2008,** *80*, 5727–5735.

(2) Hoang, T.; Roth, U.; Kowalewski, K.; Belisle, C.; Steinert, K.; Karas, M. Highly Specific Capture and Direct MALDI MS Analysis of Phosphopeptides by Zirconium Phosphonate on Self-Assembled Monolayers. *Anal. Chem.* **2010,** *82*, 219–228.

(3) Wu, H. -T.; Hsu, C. -C.; Tsai, C. -F.; Lin, P. -C.; Lin, C. -C.; Chen, Y. -J. Nanoprobe-based Immobilized Metal Affinity Chromatography for Sensitive and Complementary Enrichment of Multiply Phosphorylated Peptides. *Proteomics* **2011,** *11*, 2639–2653.

(4) Krenkova, J.; Foret, F. Iron Oxide Nanoparticle Coating of Organic Polymer-based Monolithic Columns for Phosphopeptide Enrichment. *J. Sep. Sci.* **2011,** *34*, 2106–2112.

(5) Li, X. S.; Wu, J. H.; Zhao, Y.; Zhang, W. P.; Gao, Q.; Guo, L.; Yuan, B. F.; Feng, Y. Q. Preparation of Magnetic Polymer Material with Phosphate Group and its Application to the Enrichment of Phosphopeptides. *J. Chromatogr. A.* **2011,** *1218*, 3845–3853.

(6) Krenkova, J.; Foret, F. Nanoparticle-Modified Monolithic Pipette Tips for Phosphopeptide Enrichment. *Anal. Bioanal. Chem.* **2013,** *405*, 2175–2183.

(7) Saeed, A.; Najam-ul-Haq, M.; Jabeen, F.; Svec, F. High Affinity Phosphopeptides Enrichment and Desalting of Biological Materials on Newly Engineered Poly(Glycidyl Propargyl Ether/Divinyl Benzene). *Anal. Chem.* **2013,** *85*, 8979–8986.